PAPER

NJC
www.rsc.org/njc

Large hyperpolarizabilities of trinuclear transition metal clusters $[MAg_2X_4(C_5H_5NS)(PPh_3)_2]\cdot CH_2Cl_2$ (M = Mo, W; X = S, Se): a DFT study

Kechen Wu,* Rongjian Sa and Chensheng Lin

State Key Laboratory of Structural Chemistry, Fujian Institute of Research on the Structure of Matter, Chinese Academy of Sciences, Fuzhou, Fujian, 350002, China. E-mail: wkc@ms.fjirsm.ac.cn; Fax: +86-591-83714946

Received (in Montpellier, France) 3rd July 2004, Accepted 8th September 2004
First published as an Advance Article on the web 13th January 2005

Static and dynamic first hyperpolarizabilities have been studied by a DFT approach for a series of trinuclear heterometallic transition metal molecular clusters, $[MAg_2X_4(C_5H_5NS)(PPh_3)_2]\cdot CH_2Cl_2$ (M = Mo, W; X = S, Se) with incomplete cubane-like configurations. Their nonlinear optical nature has been analyzed by using a two-level model. The large hyperpolarizabilities of about 100×10^{-30} esu of these metal clusters are generated by intermolecular charge transfers from the metal core to the pyridine-2-thiol ligand as well as by intramolecular charge transfers within the metal core. The conjoint effects of stereo π (3D) conjugation of the metal core and planar π (2D) conjugation of the C_5H_5NS ligand enhance these hyperpolarizabilities, while the presence of CH_2Cl_2 has a negative effect by lowering them. Since these complexes are all crystallized in noncentrosymmetric configurations, they are promising candidates as IR second-order nonlinear optical transition metal coordinated materials.

Introduction

Nonlinear optical (NLO) materials applied in photonics devices are extremely demanded nowadays.[1] The most intensively investigated NLO materials are inorganic oxides, organic materials, polymers and organometallic complexes.[2] More recently, transition metal clusters (TMC) have been found to represent a promising area for novel IR NLO materials,[3–6] probably due to their hybrid structures combining advantages from inorganic materials (such as colorful structures and high stability) and organic compounds (structure tailoring for large hyperpolarizabilities). Furthermore, the heavy transition metal ions used in TMC usually lead to anisotropic structures at the molecular level, beneficial to high NLO activity. The most important factor is that they are usually optoelectronically active in the spectroscopic region from the medium to far IR. This advantage makes them potential candidates for IR NLO materials, which are nowadays in great demand for developing contemporary optical communication devices.

Theoretical evaluation of NLO properties of TMC becomes accessible thanks to the fast development of density functional theory (DFT).[7,8] Some recent reports supported the efficiency and reliability of DFT calculations on TMC for establishing optical absorption spectra and NLO properties.[9–15] In this paper, a series of trinuclear transition metal clusters $[MAg_2X_4(C_5H_5NS)(PPh_3)_2]\cdot CH_2Cl_2$ (M = Mo, W; X = S, Se) with incomplete cubane-like structures have been investigated using the DFT method. The relationship between structure and NLO properties has been illustrated with the aim to better understand the NLO nature of TMC compounds. The results show that these three molecular clusters possess very large first hyperpolarizabilities (β). Charge transfer (CT) from the metal core to the organic ligands and with the metal core play a major role in hyperpolarizability enhancement.

Computational models and methods

We selected supermolecular models **1–3** for DFT calculations, each containing a neutral molecular metal cluster $[MAg_2X_4(C_5H_5NS)(PPh_3)_2]$ (M = Mo, X = S for **1**, M = W, X = S for **2**, and M = W, X = Se for **3**) and a single dichloromethane molecule. We used the isolated supermolecular computing model in order to take into consideration the contribution of CH_2Cl_2 to hyperpolarizability. Each neutral metal cluster contains a metal core $[MAg_2X_4]$ with an incomplete cubane-like configuration and three coordinated organic ligands, that is, a pyridine-2-thiol (C_5H_5NS) and two neutral PPh_3. The crystal structures of cluster complexes **1–3** are comparable to each other, being all three in a $P2_12_12_1$ noncentrosymmetry space group.[16,17] The molecular structures and Cartesian orientations of prototypal supermolecular models **1–3** are shown in Fig. 1. The geometric parameters such as bond lengths and angles are all taken from X-ray experimental data available in the literature.[16,17]

In addition, two simulated models (model **4** and **5**, Fig. 1) were designed in the following way: removal of the CH_2Cl_2 molecule in cluster **1** resulted in model **4**; replacement of the pyridine-2-thiol ligand in cluster **1** by a CH_2S ligand resulted in model **5**. The selected geometric parameters for these two simulated models have been optimized at the DFT/LDA/SVWN level.

In hyperpolarizability calculations, the generalized gradient approximation potential (GGA) with LB94 XC potentials was used.[18] The calculated static hyperpolarizabilities of clusters **1–5** are listed in Table 1 below. In both optimizations and hyperpolarizability calculations we used an unrestricted triple-ξ STO basis set extended by one polarization function for nonmetal elements P, S, Se, N, O, C and H and an unrestricted triple-ξ STO basis set extended by two additional polarization functions for transition metals. The cores (N, O, C: 1s; P, S, Cl: 2p; Se: 3d; Mo, W, Ag: 4p) were kept frozen. The conventional method reported in refs. 19–22 was used to calculate the excitation properties and optical spectrum within the TDDFT framework. Calculation of the optical spectrum was carried out only for cluster **1** because of the similarity between the three cluster prototypes. GGA/LB94 XC potentials and both basis sets mentioned above were used for the excitation calcu-

DOI: 10.1039/b410226f

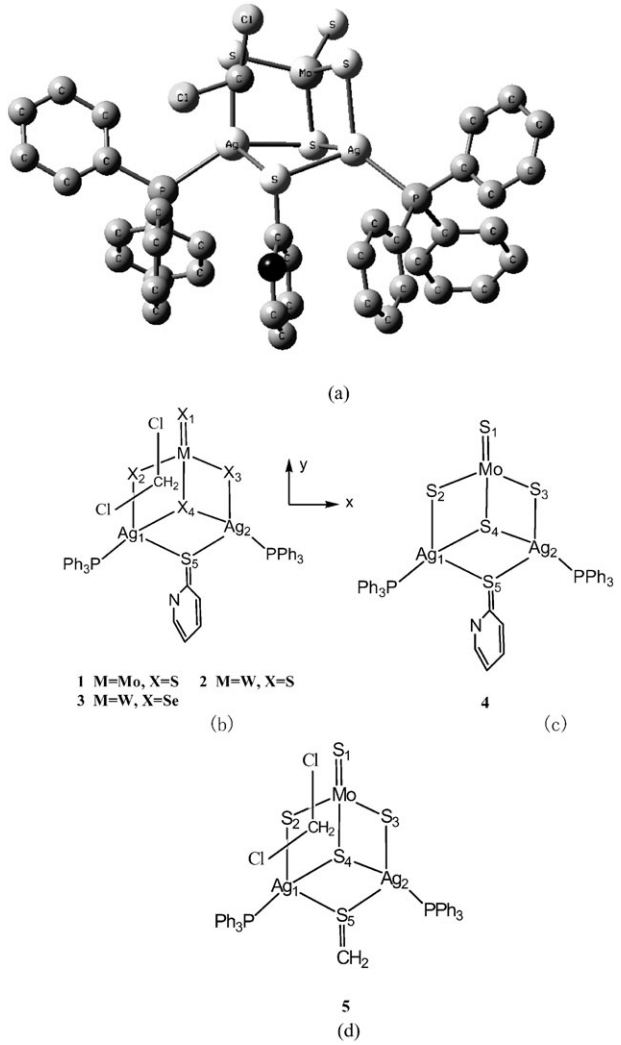

Fig. 1 Molecular structures and orientation of the model clusters. (a) Cluster **1** in a ball-and-stick representation. The hydrogen atoms are not depicted for clarity. (b) Clusters **1–3**, (c) cluster model **4** and (d) cluster model **5**.

lations. For all calculations, we adopted a scalar relativistic ZORA to take relativistic effects into account. All computational calculations were performed with the ADF 2003 program package.[23]

Results and discussion

Hyperpolarizabilities of models 1–3

All three prototypal supermolecular clusters belong to a C_1 point group symmetry. The hyperpolarizability β tensor of each supermolecular cluster thus contains 27 nonzero components. To simplify, only spatial average values $\beta_{\mathrm{av},i}$ ($i = x, y, z$) and intrinsic total hyperpolarizability β_{tot} along the i direction are listed in Table 1 for clusters **1–5**. They are defined as

Table 1 TDDFT results of the first static hyperpolarizabilities ($\times 10^{-30}$ esu) of the model clusters **1–5**

	1	2	3	4	5
$\beta_{\mathrm{av},x}$	1.5	1.3	1.8	7.9	0.8
$\beta_{av,y}$	90.0	115.2	110.9	104.5	20.0
$\beta_{\mathrm{av},z}$	−44.4	−53.9	−55.7	−55.1	−35.4
β_{tot}	100.3	127.2	124.2	118.4	40.7

Table 2 TDDFT results of the first non-resonance dynamic hyperpolarizabilities ($\times 10^{-30}$ esu, at 1.064 μm) of prototype clusters **1–3**

	1	2	3
$\beta_{\mathrm{av},x}{}^{\mathrm{d}}$	4.5	3.2	4.9
$\beta_{\mathrm{av},y}{}^{\mathrm{d}}$	110.5	135.4	128.7
$\beta_{\mathrm{av},z}{}^{\mathrm{d}}$	−64.4	−69.2	−75.3
$\beta_{\mathrm{av,tot}}{}^{\mathrm{d}}$	127.9	152.1	149.2

follows:

$$\beta_{\mathrm{av},i} = \frac{1}{3}\sum_{j}^{3}(\beta_{ijj} + \beta_{jij} + \beta_{jji}) \quad (i,j = x,y,z) \qquad (1)$$

$$\beta_{\mathrm{tot}} = \sqrt{\sum_{i}\beta_{\mathrm{av},i}^{2}} \quad (i = x,y,z) \qquad (2)$$

Extraordinarily large $\beta_{\mathrm{av},i}$ values for prototypal clusters **1–3** were observed, particularly in the y direction which runs from the metal core to the pyridine-2-thiol ligand. Indeed, $\beta_{\mathrm{av},y}$ of **1** is about 90×10^{-30} esu, that is about 2.5 times larger in magnitude than the average first hyperpolarizability of 3-methyl-4-methoxy-4′-nitrostilbene (MMONS, 38.2×10^{-30} esu by the DFT approach), MMONS crystals having the largest NLO coefficient among organic NLO crystals available to date.[24] The predicted molecular hyperpolarizabilities are very encouraging although experimental values are not available yet to support them. Since all three clusters are in an acentric space group, promising second-order NLO properties are strongly expected for these crystals.

First frequency-dependent hyperpolarizabilities (β^{d}) at 1.064 μm were also obtained by TDDFT calculations.[25] The dynamic $\beta_{\mathrm{av},i}{}^{\mathrm{d}}$ values of **1–3** are listed in Table 2. It was found that the dispersion effects of these clusters are weak.

The $\beta_{\mathrm{av},i}$ values of **1–3** are comparable, which obviously comes from the similarity between their structures. The substitution from molybdenum to tungsten and from sulfur to selenium did not give rise to a significant variation of β. The slight configuration distortion caused by atom substitutions (for example, the W–X bond length increases by ~0.13 Å from X = Se in **3** to X = S in **2**†) only contributed to a small variation of $\beta_{\mathrm{av},i}$. For example, the $\beta_{\mathrm{av},y}$ decreased from 127.2×10^{-30} esu for **2** to 124.5×10^{-30} esu for **3**.

One astonishing result is the observed anisotropy of $\beta_{\mathrm{av},i}$ values: $\beta_{\mathrm{av},y} > \beta_{\mathrm{av},z} \gg \beta_{\mathrm{av},x}$. A larger $\beta_{\mathrm{av},y}$ implies larger charge transfer in the y direction upon laser irradiation. The planar C_5H_5NS ligand is a typical π-conjugated ring system. The incomplete cubane-like $[MAg_2X_4]$ core has been reported to form a stereo-conjugated electron system by M–X–Ag d-p π bonds.[16,17] These two electron-conjugated systems, which are bridged by the μ_2-S5 atom, greatly enhance the $\beta_{\mathrm{av},y}$ value along the direction of the π backbone.

Hyperpolarizability of models 4 and 5

When comparing **4** to **1** (see Table 1), all $\beta_{\mathrm{av},i}$ values are enhanced by about 20%. Hence, a strong influence of the solvent on the hyperpolarizability is outlined as, in this case, the NLO response of prototypal cluster **1** would be improved if the dichloromethane molecules could be eliminated.

When the C_5H_5NS ligand in model **1** was replaced by a simple nonconjugated CH_2S in **5**, the $\beta_{\mathrm{av},y}$ value was reduced to less than one-fourth of that of **1**. This outlines clearly the important role of the p-π planar conjugation of the organic ring in enhancing the hyperpolarizability of prototypal clusters.

† **3**: W–Se1 = 2.265 Å; **2**: W–S1 = 2.135 Å.[16,17]

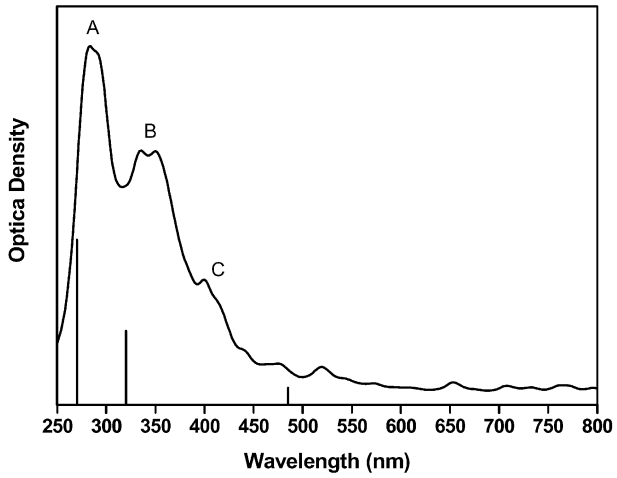

Fig. 2 Calculated optical absorption spectrum of **1** and reported[16] corresponding experimental absorption maxima (vertical lines).

Optical spectra of model 1

Two-level model [TLM, eqn. (3)] is commonly used to analyze the NLO nature of organometallic complexes and transition metal clusters.[26,27]

$$\beta_{CT} \propto \frac{\Delta\mu_{ng} f_{ng}}{\omega_{ng}^3} \qquad (3)$$

According to TLM, where f_{ng} is the oscillator strength of the transition from the ground state to the n^{th} excited state, $\Delta\mu_{ng}$ is the difference of the dipolar moment between ground state and the n^{th} excited state, and ω_{ng} is the transition frequency, β_{CT} is proportional to optical absorption and inversely proportional to the cube of the transition frequency. This indicates that strong absorption peaks with a low excitation energies would make larger contributions to β. This provides an effective way to understand the NLO nature of a material through the calculation and analysis of linear optical parameters.

A calculated absorption spectrum was recorded for cluster **1** (Fig. 2) and compared to a corresponding experimental absorption spectrum previously described in the literature.[16] **1** presents three notable absorption peaks, marked A, B and C (see Fig. 2) in the 350–700 nm range. A is an intense peak centered at 287.0 nm, which is in good agreement with the experimental strong absorption recorded at 270 nm. B is a broader signal of medium intensity composed of two neighboring peaks B_1 and B_2. B_1 is centered at 336.3 nm while B_2 is at 353.5 nm. Only one medium absorption signal located at 320 nm has been measured in the literature, probably due to resolution limitations. C is a weak peak centered at 428.6 nm. This theoretical measure is underestimated, according to the corresponding reported weak absorption observed at 485 nm.

Molecular orbital (MO) analysis was used to briefly describe CT upon electronic excitation transitions at these maxima. The excitation transition of peak A mainly arose from three following types of MO transitions: (1) transition from the MO composed of p orbitals from S atoms and d orbitals from Mo and Ag atoms in the metal core to π* orbitals from $2p_x$ orbitals of the pyridine-2-thiol ligand; (2) transition from the MO of some of the atoms of the metal core to the MO of the other atoms of the metal core; (3) transition from the MO composed of p orbitals of CH_2Cl_2 to p orbitals of the C atoms in the two PPh_3 ligands. In short, the β_{CT} contribution from peak A is related to MLCT from the metal core to pyridine-2-thiol , intra-metal-core CT and CH_2Cl_2 to $(PPh_3)_2$ ligand CT.

Peaks B1, B2 and C were analyzed similarly. B_1 and B_2 provided significant β_{CT} by MLCT from the metal core to pyridine-2-thiol, intra-metal-core CT, and MLCT from the metal core to $(PPh_3)_2$ and to CH_2Cl_2. The latter is very special,

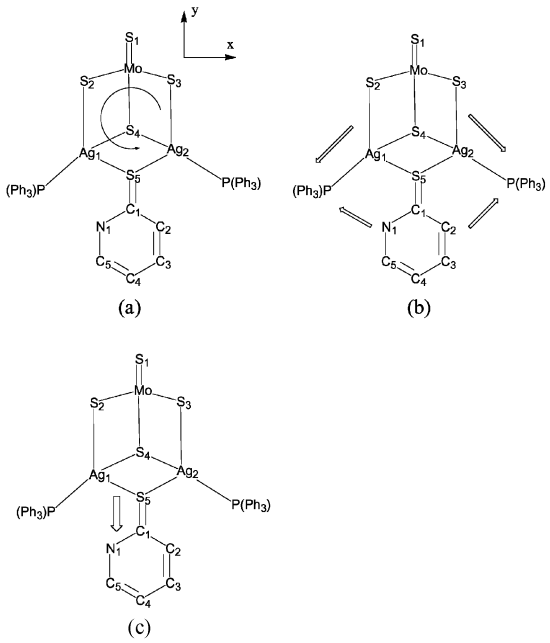

Fig. 3 Schematic representation of the main charge transfer processes in **1** upon optical excitation. (a) 3D charge transfer in the metal core; (b) symmetric charge transfer from the metal core and pyridine-2-thiol ligand to the PPh_3 ligands; (c) charge transfer from the metal core to the pyridine-2-thiol ligand along the y axis (CH_2Cl_2 and hydrogen atoms are not represented for clarity).

and since CH_2Cl_2 is located along the z axis it contributes to $\beta_{av,z}$. Finally, the contribution of the low-energy peak C to β comes from MLCT from the metal core to $(PPh_3)_2$ and to pyridine-2-tiol.

In summary, the major CT contributions to β are schematically represented in Fig. 3 and listed hereafter in decreasing order of importance: (1) metal core to pyridine-2-thiol MLCT; (2) intra-metal-core CT; (3) metal core to CH_2Cl_2 CT; (4) metal core to $(PPh_3)_2$ MLCT; (5) CH_2Cl_2 to $(PPh_3)_2$ ligand CT. Due to the symmetric distribution of PPh_3 ligands along the x axis, CT arising from processes (4) and (5) did not make any notable contribution to $\beta_{av,x}$. This explains the low values of $\beta_{av,x}$. The large $\beta_{av,z}$ values resulted from metal core to CH_2Cl_2 CT and intra-metal-core CT. The latter came from the special geometric configuration of the metal core, an incomplete cubane-like structure in which the missing cubane corner is in the z direction. The metal core to pyridine-2-thiol MLCT along the y axis is found in all three absorption peaks (A, B and C). It is obviously the most important CT process and is at the origin of the observed large $\beta_{av,y}$ values.

Conclusion

The first-principle DFT/GGA/LB94 calculations have been carried out on static first hyperpolarizabilities of three heterometallic incomplete cubane-like transition metal clusters, **1–3**. The microscopic origin of the NLO property and the relationship between structural configuration and hyperpolarizability have been discussed.

The first hyperpolarizabilities found in this series of TMC are several times larger than that of MMONS. Since all three clusters crystallize in a noncentrosymmetric space group ($P2_12_12_1$), they are promising candidates as second-order NLO materials, especially in the IR region.

The enhanced β_{tot} values originate from various CT processes. Based on the concepts of traditional D-π-A CT in organic molecules and MLCT in organometallic systems, it is understandable to find a large variety of CT processes in these multinuclear TMC. For instance, the CT from the metal core to coordinated ligands is similar to the common MLCT

observed in organometallic materials and widely described in the literature.[28] However, in addition to MLCT, one specific CT was observed in this series of metal clusters that is strongly related to the asymmetry of the structural configuration, that is, the incomplete cubane-like structure. This distinct intra-metal-cluster CT makes a great contribution to the β_{tot} values. In a previous report, we found that the hyperpolarizability of a TMC with a cubane-like symmetric structure was very small.[29] The contribution of solvent molecules to hyperpolarizability in TMC is sometimes neglected due to the obviously weak intermolecular interactions between the solvent molecule and the molecular metal cluster. However, our study shows that the contribution of CH_2Cl_2 to the hyperpolarizability of our supermolecular clusters goes far beyond expectation. Further work on the effect of weak van der Waals intermolecular interactions on CT mechanisms (such as, for example, Onsager solvent effect studies) would be beneficial to both NLO material science and supermolecular chemistry.

To conclude, our study suggested that (1) both coordinate ligands and coordinate sites of the metal core should be carefully selected (completely different contributions to β_{tot} from PPh_3 and pyridine-2-thiol was observed here); (2) the hyperpolarizabilities of a molecular cluster are very sensitive to the structural configuration of the metal core; (3) the selection of solvent molecules should be carefully addressed because it may reduce (like CH_2Cl_2 in this report) or enhance the hyperpolarizability. An in-depth understanding of the NLO nature of TMCs is still missing. The results of this study may be helpful for further advances in this area.

Acknowledgements

We are grateful to Professor Dr J. G. Snijders for useful discussions, kind revisions and sincere help. The study was financially supported by National Science Foundation of China, grants 69978021, 20173064 and 90203017.

References

1 S. P. Karna, *J. Phys. Chem. A*, 2000, **104**, 4671.
2 D. M. Burland, *Chem. Rev.*, 1994, **94**, 1–2.
3 *Optoelectronic Properties of Inorganic Compounds*, eds. D. M. Roundhill and J. P. Fackler Jr, Academic Press, New York, 1998.
4 R. Phillip, G. R. Kumar, P. Mathur and S. Ghose, *Opt. Commun.*, 2000, **178**, 469.
5 C. Lambert, W. Gaschler, M. Zabel, R. Matschiner and R. Wortmann, *J. Organomet. Chem.*, 1999, **592**, 109.
6 X. Chen, K. Wu, J. G. Snijders and C. Lin, *Inorg. Chem.*, 2003, **42**, 532.
7 N. Matsuzawa, J. Seto and D. A. Dixon, *J. Phys. Chem. A*, 1997, **101**, 9391.
8 E. R. Davidson, *Chem. Rev.*, 2000, **100**, 351.
9 G. Ricciardi, A. Rosa, S. J. A. van Gisbergen and E. J. Baerends, *J. Phys. Chem. A*, 2000, **104**, 635.
10 C. Lin, K. Wu, J. G. Snijders, R. Sa and X. Chen, *Acta Chim. Sinica*, 2002, **60**, 664.
11 G. Ricciardi, A. Rosa, E. J. Baerends and S. A. J. van Gisbergen, *J. Am. Chem. Soc.*, 2002, **124**, 12319.
12 V. Cavillot and B. Champagne, *Chem. Phys. Lett.*, 2002, **354**, 449.
13 P. J. Hay, *J. Phys. Chem. A*, 2002, **106**, 1634.
14 Y. Yamaguchi, *J. Chem. Phys.*, 2002, **117**, 9688.
15 Y. Q. Qiu, Z. M. Su, L. K. Yan, Y. Liao, M. Zhang and R. S. Wang, *Synth. Met.*, 2003, **137**, 1523.
16 Q. Wang, X. Wu, Q. Huang, T. Sheng and P. Lin, *Polyhedron*, 1997, **16**, 1543.
17 Q. Wang, X. Wu, Q. Huang and T. Sheng, *J. Cluster Sci.*, 1996, **7**, 371.
18 R. van Leeuwen and E. J. Baerends, *Phys. Rev. A*, 1994, **49**, 2421.
19 M. Casida, in *Recent Advances in Density Functional Methods*, ed. D. P. Chong, World Scientific, Singapore, 1995, **vol. 1**, 155–156.
20 C. Jamorski, M. Casida and D. R. Salahub, *J. Chem. Phys.*, 1996, **104**, 5134.
21 R. Bauerschmitt and R. Ahlrichs, *Chem. Phys. Lett.*, 1996, **256**, 454.
22 A. Rosa, E. J. Baerends, S. A. J. van Gisbergen, E. Vanlenthe and J. A. Groeneveld, *J. Am. Chem. Soc.*, 1999, **121**, 10356.
23 (*a*) C. Fonseca Guerra, O. Visser, J. G. Snijders, G. te Velde and E. J. Baerends, in *Methods and Techniques for Computational Chemistry*, eds. E. Clementi and C. Corongiu, STEF, Calgary, 1995, pp. 303–395; (*b*) G. te Velde, F. M. Bickelhaupt, E. J. Baerends, S. J. A. van Gisbergen, C. F. Fonseca Guerra, J. G. Snijders and T. J. Ziegler, *J. Comput. Chem.*, 2001, **22**, 931.
24 J. D. Bierlein, L. K. Cheng, Y. Wang and W. Tam, *Appl. Phys. Lett.*, 1990, **56**, 423.
25 S. J. A. van Gisbergen, J. G. Snijders and E. J. Baerends, *Comput. Phys. Commun.*, 1999, **118**, 119.
26 S. Di Bella and I. Fragalà, *New J. Chem.*, 2002, **26**, 285.
27 D. R. Kanis, M. A. Ratner and T. J. Marks, *J. Am. Chem. Soc.*, 1992, **114**, 10338.
28 For example: H. Le Bozec and T. Renouard, *Eur. J. Inorg. Chem.*, 2000, **2**, 229.
29 R. Sa, K. Wu, P. Liu, C. Lin and C. Mang, *Chin. Chem. Lett.*, 2002, **13**, 1205.